

The Effects of Stirring Speed on Coupled Transport of Nitrite Ions Through Liquid Membranes

N. Demircioğlu, M. Levent*, M. Kobya**, and N. Topçu***

Department of Environmental Engineering, Faculty of Engineering,
Atatürk University, 25240 Erzurum, Turkey

*Department of Chemical Engineering, Faculty of Engineering,
Atatürk University, 25240 Erzurum, Turkey

**Department of Environmental Engineering,
Gebze Yüksek Teknoloji Enstitüsü, İzmit, Turkey

***Department of Environmental Engineering, Faculty of Engineering,
Süleyman Demirel University, İsparta, Turkey

Original scientific paper

Received: 4. 2. 2000.

Accepted: 6. 9. 2000.

In this study, the effects of stirring speed on coupled transport of nitrite ions through liquid membranes has been investigated at various stirring speeds in the range of 100–250 rpm. Coupled transport of nitrite ions through liquid membranes ($\varphi = 85\%$ hexane + $\varphi = 15\%$ trichlorometane) containing tetraoctyl ammonium chloride (TOACl) as a carrier, was examined. For the diffusion of the nitrite ion-carrier complex at various stirring speeds through the narrow boundary layers at the interface of the membrane, the variable membrane entrance (k_{1d}) and exit rates (k_{2m} and k_{2a}) are the rate determining steps. The activation energies of membrane entrance and exit permeate rates for nitrite ions are $E_{am} = 1.58$ and $E_{aa} = 1.583$ kJ mol⁻¹, respectively. From these experimental results, it was concluded that the reaction was diffusion controlled. The membrane was stable during the transport experiments (no leakage of carrier and carrier-nitrite ion complexes to both aqueous phases and also there was no supplementary water penetration into the membrane was observed). This favours the interfacial character of nitrite ion-carrier complexation reaction.

Keywords:

Coupled transport, nitrite ion transport, non-steady state kinetics, bulk membrane stability, rate determination step.

Introduction

In recent years, new and interesting developments have been developed for the separation of ions and molecules from wastewater. Membrane processes have been often used in usual separation processes. Usual separating operations in the area of separation sciences are solvent extraction, ion exchange etc. Beside of these conventional separating operations, ultrafiltration, hiperfiltration, microfiltration, reverse osmosis, dialyse, electro dialyse and liquid membranes are used as important separation techniques as well (Winston Ho and Sirkar, 1992).¹

It is well known, that polymeric and liquid membranes are often used in molecule and ion transportation processes. However, some properties of polymeric membranes such as higher energy costs, lower permeation rate and selectivity limit the use of these types of membranes. The high selectivities permeation and separating efficiencies of liquid membranes are very important from the point of technological practice. Liquid membranes have broad application areas such as; gas treatment and purification, removal of toxic components, separation of fermentation products

and wastewater treatment (Noble and Way, 1989; Mulder, 1990).^{2,3}

In spite of many examples in the literature on cation separation, only few investigations on anion separation are known (Molnar, et al., 1978; Sugiura and Yamaguchi, 1983).^{4,5} High nitrite ion concentrations are present in industrial wastes of iron, steel, explosive production in municipal wastewater, as well as in agriculture wastes. The maximum permissible limit of nitrite for drinking water is about 0.1 mg l⁻¹ in EEC countries. These ions are removed from waste water by chemical precipitation, ion exchange, reverse osmosis, electro dialysis, biological denitrification, and ultrafiltration processes (Dahab, 1992; Patterson, 1985; Francis and Callahan, 1975; İldiz, et al., 1996).^{6,7,8}

Besides these techniques, it has been thought that nitrite removal by liquid membranes is an interesting method. In this study, the removal of nitrite ions from aqueous streams with liquid membrane technique, has been investigated. Among the other quantities (temperature, pH, acceptor phase type and medium concentration), the stirring speed was chosen as process parameter. From the experimental results, it has been determined

that the reaction was diffusion controlled. The transport efficiency of nitrite ions increased with increasing stirring speed. The membrane entrance and exit rate constants (k_{1d} , k_{2m} and k_{2a} , respectively) were linearly dependent on the stirring speeds of 100 to 250 rpm.

Experimental

Material

Tetraoctyl ammonium chloride (TOACl) was used as a carrier in coupled transport of nitrite ions with the carrier concentration of 10^{-3} mol l⁻¹. The carrier was dissolved in hexane (Merck, >99%) and trichloromethane (Merck, >99%). In donor phase NaNO₂ (Merck, >99%), and in acceptor phase, the concentrated CaCl₂ (Merck, > 99%) was used.

Kinetic Procedure

The experiments of coupled transport of nitrite ions experiments were conducted in a reactor shown in Fig. 1. The three phases, the donor (d), the membrane (m) and the acceptor (a) phases, were applied in the reactor. 75 ml CaCl₂ (2 mol l⁻¹) solution was put into the inner and 75 ml nitrite ($c_{d0} = 3.09.1 \times 10^{-3}$ mol l⁻¹) solution was put into the outer reactor, and to the surface of these, 200 ml organic (membrane) phase with a carrier concentration of 10^{-3} mol l⁻¹. The organic (membrane) phase contains 85% hexane and 15% trichloromethane and has a density less than 1 ($\rho < 1$).

The coupled transport experiments were carried out at 25 ± 0.2 °C with a thermostat (Techne Mark, Model TE-8D). Organic membrane phase was stirred by a digital mechanical stirrer (IKA Werk Mark, Model RE-166), and the donor and acceptor phases were stirred by a digital magnetic stirrer (Heidolph Mark, Model MR 3003 SD). Mixing speeds of donor and acceptor phases were

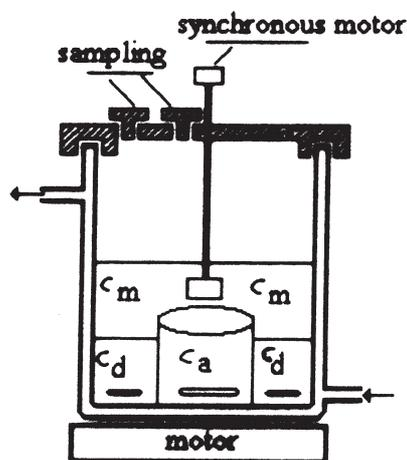


Fig. 1 – The experimental set up for coupled transport with liquid membranes

150 and 200 rpm, respectively. But, the mixing speeds of organic membrane phase (ω_m) were varied in the range of 50–250 rpm. The interface surfaces amounted; $S_{dp/memb.} = 36.37$ cm², $S_{ap/memb.} = 17.32$ cm². The samples (about 0.5 ml) were taken from both aqueous phases (d and a) in 30 minutes time intervals and the nitrite analysis were carried out by an UV 160 A, Shimadzu model spectrophotometer.

Coupled transport kinetic of nitrite ions with liquid membranes

For modelling and design of transport processes, the determination of the rate controlling step is very important. It is generally accepted that the following particular steps are involved in a transport process through a stirred liquid membrane system (Fig.2). It is assumed that transport across the liquid membrane consists of the following steps:

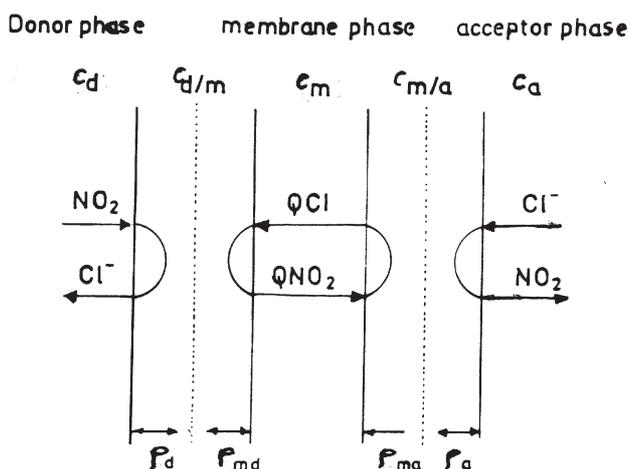


Fig. 2 – A schematic view of coupled transport of nitrite ions with liquid membrane system

- The diffusion of carrier molecules from the donor phase to the membrane-donor interface (c_m/c_d).
- The diffusion of molecules from membrane phase to membrane-donor interface (c_m/c_d).
- The adsorption of the membrane donor interface (c_m/c_d) molecules at interface (c_m/c_d).
- The complex formation (QNO_2) of carrier molecules with nitrite ions at donor-membrane interface (c_d/c_m) and release of cations.
- The movement of QNO_2 complex from the donor-membrane interface (c_d/c_m) to the membrane interface.
- The diffusion of QNO_2 complex to membrane phase over δ_{md} distance.
- The convective transport of QNO_2 complex across the membrane phase.

h) The diffusion of QNO_2 complex to δ_{ma} distance to the c_m/c_a interface.

i) The adsorption of QNO_2 complex at the c_m/c_a interface.

j) Decomposition of QNO_2 complex at the interface c_m/c_a .

k) Desorption of carrier molecules from the c_m/c_a interface.

l) The back diffusion of carrier molecules at membrane phase into membrane, from δ_{ma} along δ_a into the acceptor phase.

m) The transport of NO_2 ion to acceptor phase from δ_a distance.

According to these steps, at coupled transport, the (a), (b), (f), (h), (i) and (m) steps have not any effect on transport kinetics. The different diffusion steps of (b), (f), (h) and (e), and the diffusion of QNO_2 complex steps in membrane are very slow. But, the complex forming and the decomposition reactions in steps, (c), (e), (i) and (k) are very fast (Demircioğlu, 1996). To minimise the diffusion effect, the stirrer speed was increased. However, at high stirrer speeds the interface stability and the area of the interface were changed. Therefore the interfacial area was determined at 300 rpm.

In coupled transport, the carrier agent couples the flow of two or more species, e.g. nitrite ion and chloride ions. In this case, the carrier must contain, of course, chloride-ionizable groups. In this coupling, nitrite ion can be transported against its concentration gradient provided the concentration gradient of chlorides is sufficiently large. The mechanism of coupled transport of nitrite ion is given in Fig. 2.

QCl represents the chloride carrier complex. At the interface d/m, nitrite ion reacts with one chloride carrier molecule QCl , liberating one chloride ions. Then the complex, QNO_2 , diffuses through the membrane. At the interface c_m/c_a , the carrier molecules are protonated and the nitrite ions are liberated into the receiving phase. Finally, the neutral carrier diffuses back across the membrane. Thus, the nitrite ions move from left to right and electrical neutrality is maintained by the movement of chloride ions in the opposite direction.

A simple theoretical approach can be used to obtain flux equation for coupled-transport systems (Kobya, 1996);¹⁰ we must consider the equilibrium existing at the two interfaces (membrane-water phases):



The equilibrium constant of this reaction can be written as:

$$K = \frac{[\text{QNO}_2][\text{Cl}^-]}{[\text{QCl}^-][\text{NO}_2^-]} \quad (2)$$

It should be noted that only $[\text{QNO}_2]$ and $[\text{QCl}]$ are measurable in the organic phase (phase m) and $[\text{Cl}^-]$ and $[\text{NO}_2^-]$, in the aqueous phases (d and a). Taking into account Fick's law at steady state, the flux of the nitrite complex across the liquid membrane is given by:

$$J_{\text{QNO}_2} = \frac{D_{\text{QNO}_2}}{\delta} ([\text{QNO}_2]_d - [\text{QNO}_2]_a) \quad (3)$$

where D_{QNO_2} is the mean diffusion coefficient of the complex in the water-membrane interface of thickness δ . The coupling effects can be demonstrated by taking into account the mass-balance expression for the carrier molecule:

$$[\text{QNO}_2] + [\text{QCl}] = c \quad (4)$$

where c is the total concentration of the pure carrier QCl . By combining Eqs. (2)-(4), we obtain the final flux equation:

$$J = \frac{D}{\delta} c \left[\left(\frac{1}{1 + \frac{[\text{Cl}^-]}{K[\text{NO}_2^-}]_d}} \right) - \left(\frac{1}{1 - \frac{[\text{Cl}^-]}{K[\text{NO}_2^-}]_a} \right) \right] \quad (5)$$

It can be seen that active transport will exist as long as we have

$$\left(\frac{[\text{Cl}^-]}{K[\text{QCl}][\text{NO}_2^-]} \right)_d < \left(\frac{[\text{Cl}^-]}{K[\text{QCl}][\text{NO}_2^-]} \right)_a \quad (6)$$

i.e.

$$\frac{[\text{NO}_2^-]_d}{[\text{NO}_2^-]_a} > \frac{[\text{Cl}^-]_d}{[\text{Cl}^-]_a} \quad (7)$$

The maximum separation is attained when the flux stops, i.e. when

$$\frac{[\text{NO}_2^-]_d}{[\text{NO}_2^-]_a} = \frac{[\text{Cl}^-]_d}{[\text{Cl}^-]_a} \quad (8)$$

The variation of nitrite ion concentration with time was directly measured in both donor (c_d in mol l⁻¹) and acceptor (c_a in mol l⁻¹) aqueous phases, while the corresponding time dependence in the membrane phase (c_m in mol l⁻¹) was calculated from the material balance.

Numerical analysis of kinetic parameters

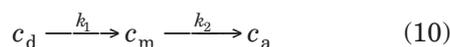
At time, t , the nitrite ion concentrations in donor, membrane and acceptor phases are named c_d , c_m and c_a , respectively, and the concentration

was given as c_{d0} in donor phase for $t = 0$. Since the concentration changes are very small, it was thought that writing in R notation is more practical so, which has also dimensionless unit.

In this case the reduced concentrations can be written as follows;

$$R_d = \frac{c_d}{c_{d0}}, \quad R_m = \frac{c_m}{c_{d0}}, \quad R_a = \frac{c_a}{c_{d0}} \quad (9)$$

During the experiments, the samples were taken from donor and aqueous acceptor phases at regular time intervals and the changes in nitrite ion concentration were observed. The variation in membrane phase was seen as $R_d + R_m + R_a = 1$. In all cases, R_d decreases mono-exponentially with time, R_a follows a monotonically increasing sigmoid-type curve, while the time evolution of R_m presents a maximum. This means that nitrite ion transport obeys the two consecutive irreversible first order reaction according to the kinetic scheme as given below:



Where c_d , c_m and c_a represent the nitrite ion (NO_2^-) concentration in donor, membrane and acceptor phases, respectively. The irreversibility is suggested by the fact that in favorable cases, R_d and R_m are approaching zero while R_a reaches the limiting value of 1 at the end of the transport experiments (450 min, also see below). In other words, the transport from the donor phase to the acceptor phase is virtually complete without any back leakage due to kinetic reversibility. This fact could be further confirmed by the chloride material balance. As a matter of fact, the final chloride ion concentration value in the donor phase corresponded exactly to the amount of transported nitrite ions. Since these latter ions are complexed by two carrier molecules (Kobya, 1996)¹⁰, the complete transport of a given number of ion-grams of nitrite was accompanied by twice greater a number of counter-transported ion-grams of chloride. The kinetic irreversibility of the whole transport process is imposed by the important chloride gradient across the membrane, since we have $[\text{Cl}^-]_{a0}/[\text{Cl}^-]_{d0} = 5 \times 10^5$ at $t = 0$. The resulting chloride flux is coupled to the nitrite ion flux through the ionizable carrier molecules. It was shown Eq. (7) that, for steady state situation, coupled transport is maintained. It is clear from the experimental conditions that this relationship is verified in the present case, even at the transport yield of 99.99 %. Obviously, we can write

$$\frac{[\text{NO}_2^-]_{d0} - [\text{NO}_2^-]_a}{[\text{NO}_2^-]_a} > \frac{([\text{Cl}^-]_{d0} + [\text{NO}_2^-]_a)}{([\text{Cl}^-]_{a0} + [\text{NO}_2^-]_a)} \quad (11)$$

with $[\text{NO}_2^-]_{d0} = 1.09 \times 10^{-3} \text{ mol l}^{-1}$, $[\text{Cl}^-]_{d0} = 1 \times 10^{-4} \text{ mol l}^{-1}$, $[\text{Cl}^-]_{a0} = 4 \text{ mol l}^{-1}$ and $[\text{NO}_2^-]_a = 0.9966[\text{NO}_2^-]_{d0}$, from which we obtain $1 \times 10^{-3} > 2.22 \times 10^{-4}$, i.e. the transport of nitrite ion from the donor phase still continues. It can be expressed in Eq. (8) that the nitrite ion flux stops. In this case, this will occur when we have 99.96 % < transport yield (%) < 99.996 %. Therefore, it can be safely concluded that, for all practical purposes, the transport is complete and irreversible.

The k_1 and k_2 are membrane entrance and exit rate constants. The below kinetic equations can be written on the basis of above kinetic analysis;

$$\frac{dR_d}{dt} = -k_1 R_d \quad (12)$$

$$\frac{dR_m}{dt} = k_1 R_d - k_2 R_m \quad (13)$$

$$\frac{dR_a}{dt} = k_2 R_m \quad (14)$$

If the differential equations (12), (13) and (14) are integrated, as a result of that, the below equations are obtained.

$$R_d = \exp(-k_1 t) \quad (15)$$

$$R_m = \frac{k_1}{k_2 - k_1} [\exp(-k_1 t) - \exp(-k_2 t)] \quad (16)$$

$$R_a = 1 - \frac{1}{k_2 - k_1} [k_2 \exp(-k_1 t) - k_1 \exp(-k_2 t)] \quad (17)$$

where k_1 (k_{1d}) and k_2 (k_{2m} , k_{2a}) are the apparent membrane entrance and exit rate constants, respectively.

It is apparent that R_d decreases mono-exponentially with time, R_a follows a monotonically increasing sigmoid-type curve, while the time variation of R_m presents a maximum. The maximum value of R_m (when $dR_m/dt = 0$),

$$R_m^{\max} = \left(\frac{k_1}{k_2} \right)^{-k_2/(k_1 - k_2)} \quad (18)$$

If the logarithm of Eq. (18) is taken and the result is rearranged, the following equation will be obtained:

$$t_{\max} = \left(\frac{1}{k_1 - k_2} \right) \ln \left(\frac{k_1}{k_2} \right) \quad (19)$$

The actual numerical analysis was carried out by non-linear curve fitting using a BASIC iteration programme. The first rate constant, k_1 , was obtained from Eq. (15) using the donor-phase data (k_{1d}), while the membrane exit-rate constant, k_2 , may be obtained either directly from the accep-

Table 1 – Kinetic parameters for coupled transport of nitrite ions through liquid membranes at different stirring speeds.

| ω (rpm) | $k_{1d} \cdot 10^3$ (dak ⁻¹) | $k_{2m} \cdot 10^3$ (dak ⁻¹) | $k_{2a} \cdot 10^3$ (dak ⁻¹) | $R_{m,max}$ | t_{max} (dak) | k_{1d}/k_{2m} |
|-------------------|---|---|---|-------------|--------------------|-----------------|
| 50 | 3.3737 | 3.1058 | 3.1950 | 0.3832 | 308.84 | 1.0862 |
| 100 | 5.9509 | 3.9852 | 4.0433 | 0.4436 | 203.97 | 1.4933 |
| 150 | 8.0217 | 4.8895 | 4.9071 | 0.4617 | 158.06 | 1.6406 |
| 200 | 9.9104 | 5.2777 | 5.4105 | 0.5143 | 136.01 | 1.8778 |

tor-phase kinetic data (k_{2a}) using Eq. (17) or indirectly from the membrane-phase data calculated on the basis of Eq. (16) (k_{2m}). In both cases, the k_{1d} value obtained from Eq. (15) was used in calculations. The obtained kinetic parameters values, k_{1d} , k_{2m} , k_{2a} , t_{max} , R_{max} , k_{1d}/k_{2m} are given in Table 1.

Results and discussions

All of the experimental determinations of organic membrane phase have been made at similar experimental conditions, except the mixing velocity. Typical kinetic curves for donor, membrane and acceptor phases are given in Fig. 3. As can be seen in this figure, the theoretical and experimental values are in good agreement (within 15 %, approximately). Figs. 3 and 6 show that nitrite ion accumulates in the membrane phase during the transport process. As a consequence, the nitrite ion concentration gradient varies permanently and, therefore, non-steady-state kinetics will govern the whole transport process. Such kinetic behavior may be observed whenever the amounts of carrier and that of nitrite ion are comparable (Fyles, et al., 1981; Szpakowska and Nagy, 1991).¹²

The time dependence of reduced nitrite ion concentration with time in donor, membrane and acceptor phases was shown in Figs. 3, 4, 5 and 6, respectively. Coupled transport of nitrite ion experiments was executed at stirring speeds 50, 100, 150, 200 rpm. R_d decreases with time increasing the stirring speeds; at the other stirring speeds except for 50 rpm, it was realised that a large amount of nitrite ion has penetrated into the membrane phase at ~ 200 min.

The determined rate coefficients, (k_{1d} , k_{2m} and k_{2a}) at various stirring speeds are shown in Figures 7 to 9, respectively. As shown in Figures 7 to 9 the rate coefficients, (k_{1d} , k_{2m} and k_{2a}) changed linearly with stirring speeds. The experiments had been carried out in stirring speeds range of 50–250 rpm (Demircioğlu, 1996).¹³ As

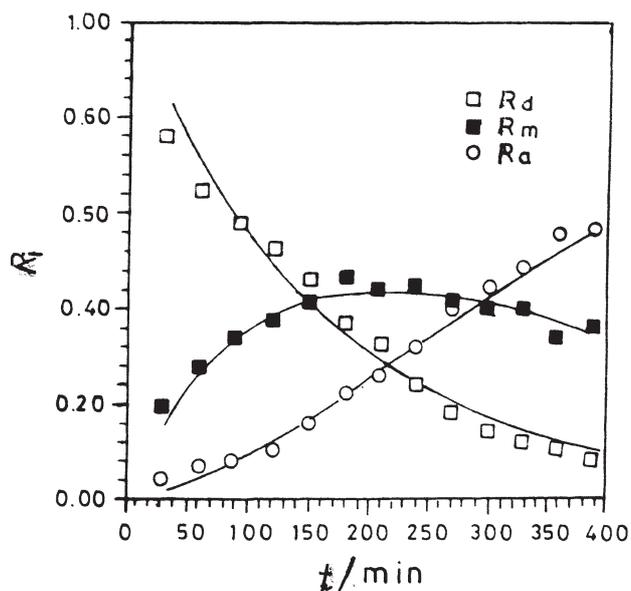


Fig. 3 – Time dependence of reduced concentration of nitrite ions, R_d (□), R_m (■), R_a (○) phases in coupled transport through liquid membranes ($T = 298 \pm 0.1$ K). Theoretical curves are calculated from eqns. (15), (16) and (17), respectively

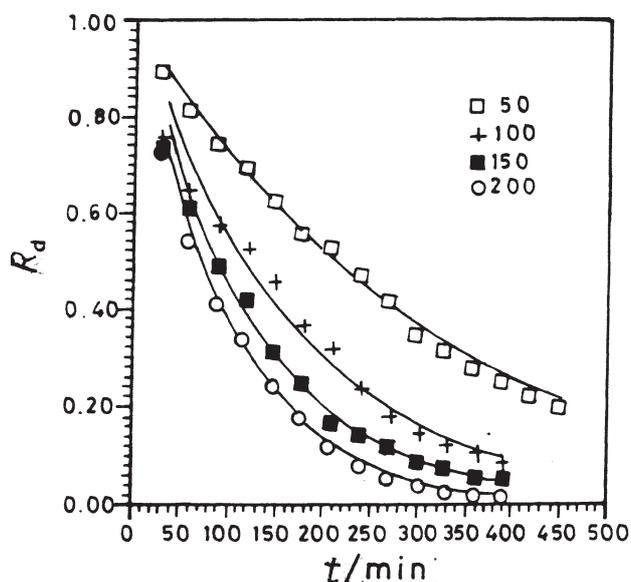


Fig. 4 – Time variation of reduced concentration of nitrite ions in the donor phase (R_d) during coupled transport through liquid membranes at different stirring speeds: 50 rpm (□), 100 rpm (+), 150 rpm (■), 200 rpm (○). Theoretical curves are calculated from Eq.(15)

can be seen from Figs. 7–9, stirring speed has a linear affect on the transport rate coefficients.

Danesi and Chiarizia (1980)¹⁴ examined similarly two phases limited conditions within diffusional and kinetical area in a two phases extraction process. In the first situation, when hydrodynamic behaviour of apparatus is well lim-

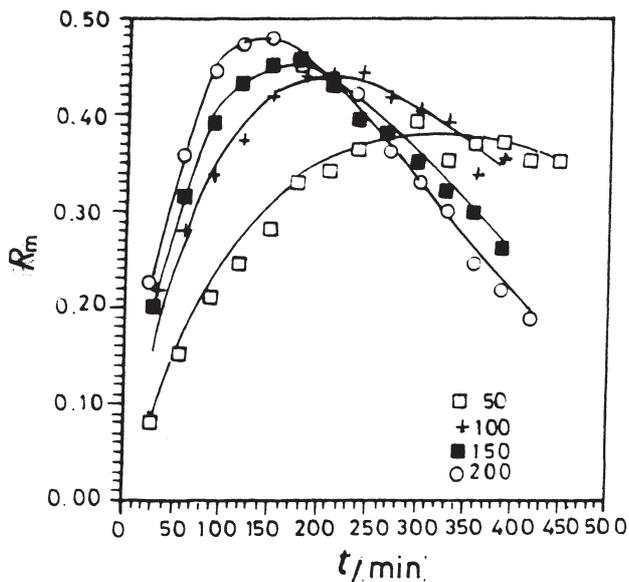


Fig. 5 - Time variation of reduced concentration of nitrite ions in the membrane phase (R_m) during coupled transport through liquid membranes at different stirring speeds: 50 rpm (□), 100 rpm (+), 150 rpm (■), 200 rpm (○). Theoretical curves are calculated from Eq. (16)

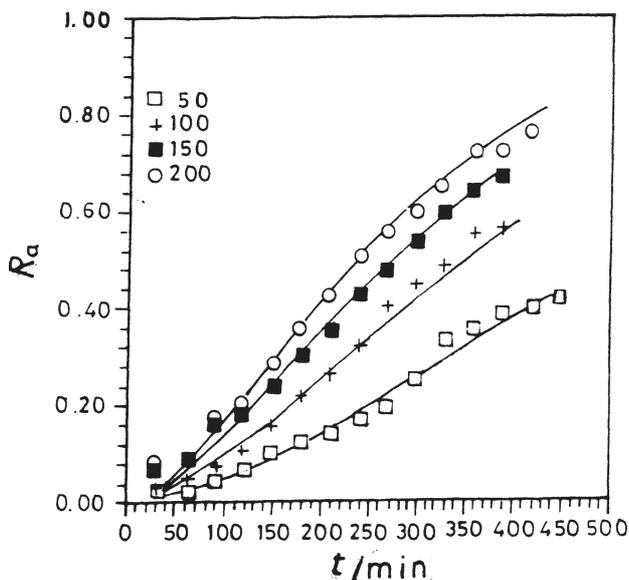


Fig. 6 - Time variation of reduced concentration of nitrite ions in the acceptor phase (R_a) during coupled transport through liquid membranes at different stirring speeds: 50 rpm (□), 100 rpm (+), 150 rpm (■), 200 rpm (○). Theoretical curves are calculated from Eq. (17)

ited, then the extraction rate is a linear function of mixing velocity. In the second situation, if transport rate is independent from mixing velocity, then the rate is constant.

In our experimental system, the organic membrane phase is positioned at the top of the donor and acceptor phases. At higher stirring speeds, the interfaces ripped up and hydrody-

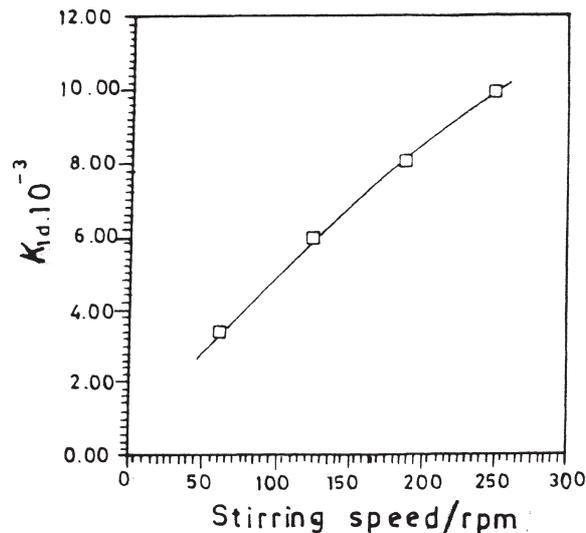


Fig. 7 - k_{1d} for nitrite ions at different stirring speeds

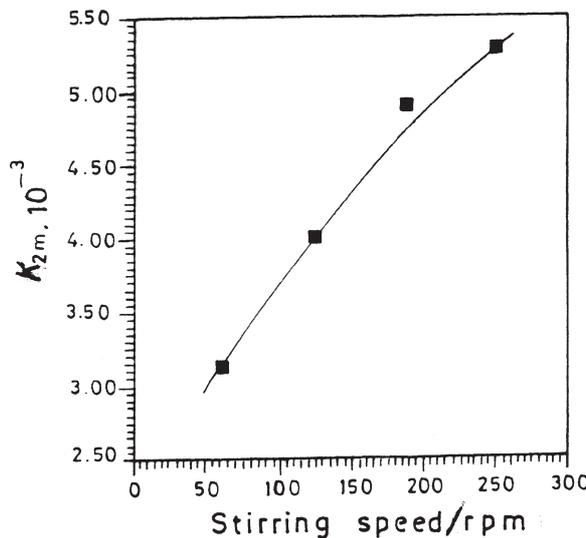


Fig. 8 - k_{2m} for nitrite ions at different stirring speeds

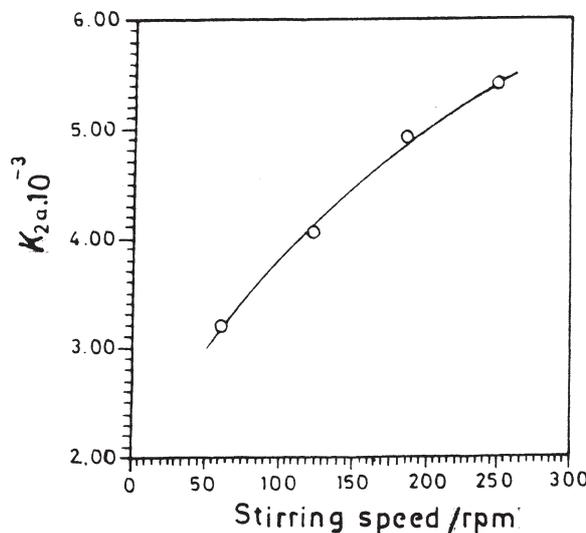


Fig. 9 - k_{2a} for nitrite ions at different stirring speeds

dynamic instabilities prevailed. At higher stirring speeds (above 350 rpm), the phases are dispersed and the interfaces between donor and acceptor phases are increased. In experiments carried out with appropriate stirring speeds, the thickness of boundary layer between donor and acceptor phases are reduced and an increase of transport efficiency of nitrite ions has been found. At various stirring speeds of donor, membrane and acceptor phases, the nitrite ion concentrations versus time are shown in Figs. 3 to 6. As can be seen from these figures, the experimental data and theoretical curves are in a good agreement.

At high stirrer speed not only the hydrodynamic instabilities at the membrane-water interface arose, but a part of the carrier was lost. This carrier penetration confer adverse effect on transport efficiency. Before and after the transport experiments, a mixture of samples of donor, membrane and acceptor phases was analysed to control this phenomenon.

The rate determining step is the diffusion of the carrier nitrite complex (QNO_2) across the thin δ_{md} to δ_{ma} film layers. The thickness of these layers is decreased with increasing stirring speeds. Transport rate can be controlled by maintaining an appropriate thickness of these layers. At higher stirring speeds ($\omega = 350$ rpm), the phases are mixed with each other and the laminar boundary layers disappear. This case has been discussed also in some other papers (Fyles, 1981; Alberly and Chouder, 1988; Szpakowska, 1994).^{11,15,16} The interfaces are ripped up in coupled transport system at higher stirring speeds ($\omega = 350$ rpm). Therefore, higher stirring speeds are not appropriate in such transport systems (Demircioğlu, 1996).¹³

UV spectrum of hexane $\varphi = 85\%$ + trichloromethane $\varphi = 15\%$ suspension which was contained in the carrier, (TOACl) is shown in Fig. 10. According to this figure, maximum wavelength (λ) is 235 nm and extinction coefficient (ϵ) is 2.2×10^3 . In the membrane phase the carrier (TOACl), was completely complexed. Its UV spectrum was shown in Fig. 10 with a wave length of 225 nm and $\epsilon = 1.6 \times 10^4$. When transport of nitrite ions was completed in donor phase, the samples were taken from donor and acceptor aqueous phases and analysed by the UV spectrophotometer (see Fig. 10 the spectrum c and d). For acceptor phase, nitrite ion and CaCl_2 concentrations were prepared from suitable KNO_3 suspension and analysed (see Fig. 10, spectrum e). As can be seen in Fig.10, the spectrums c and e, are exactly similar. This case has proved the absence of carrier and QNO_2 complexes at the end of the experiments. This observation is similar, also, for donor phase. In addition to this, non-existence of carrier molecules in donor and acceptor phases has shown, that complex reactions (formed between nitrite ion and carrier molecules) have not formed and generally, the reactions between carrier molecules occurred in water phase (Akiba and Freiser, 1982).¹⁷

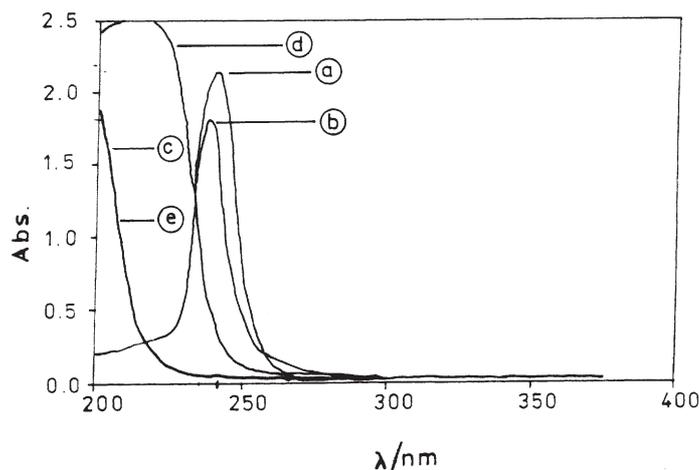


Fig. 10 – UV spectrum of phases in transport phenomena of nitrite ions: TOACl in 15 % CHCl_3 + 85 % C_6H_{14} , $C_{\text{carrier}} = 1 \times 10^{-3} \text{ mol l}^{-1}$; (b) QNO_2 complex in 15 % CHCl_3 + 85 % C_6H_{14} (liquid membrane). Nitrite concentration, $c_{\text{NO}_2^-} = 1.09 \times 10^{-3} \text{ mol l}^{-1}$; (c) Acceptor phase at the end of transport process, $c_{\text{NO}_2^-} = 4.79 \times 10^{-4} \text{ mol l}^{-1}$, $2 \text{ mol l}^{-1} \text{ CaCl}_2$; (d) $c_{\text{NO}_2^-} \text{ mol l}^{-1}$, pH 1.25 aqueous NaNO_2 solution in $2 \text{ mol l}^{-1} \text{ CaCl}_2$, $c_{\text{NO}_2^-} \text{ mol l}^{-1}$

Conclusions

As a result of the this experimental study and according to the obtained values of kinetical parameters, it was proved that stirring speed has a linear effect on coupled transport of nitrite ions. In such transport systems, the rate limiting steps are the diffusion of nitrite carrier complex (QNO_2) into δ_{md} and δ_{ma} film layers. In coupled transport system, the interfaces between phases are deformed and decomposed at higher stirring speeds greater than 350 rpm. So, the high stirring speeds are not appropriate for removal of nitrite ions from aqueous water solutions in these kind of transport systems.

When figure 10 is examined, it can be seen that, in acceptor phase, neither carrier nor carrier nitrite complex were existent at the end of the experiments. This observation holds true also for donor phase. The absence of TOACl carrier in both aqueous phases indicates that TOACl is well kept organic phase, and does not dissolve in the aqueous phase. As a result of this observation, we can state, that the transport reaction of nitrite ion is occurred between aqueous phase and membrane interface.

Nomenclature

- c – the total concentration of the pure carrier QCl , mol l^{-1}
- c_a – nitrite ion concentration in acceptor phase, mol l^{-1}
- c_d – nitrite ion concentration in donor phase, mol l^{-1}
- c_m – nitrite ion concentration in organic(membrane) phase, mol l^{-1}
- c_{d0} – initial nitrite ion concentration in donor phase, mol l^{-1}

- c_{carrier} – carrier concentration, mol l⁻¹
 D_{QNO_2} – mean diff. coeff. of the complex in the memb. of thickness δ , m² s⁻¹
 E_a – activation energy, kJ mol⁻¹
 J_{QNO_2} – the flux of the nitrite complex across the liquid membrane, min⁻¹
 K – equilibrium constant, dimensionless
 k_1 – membrane entrance rate constant, min⁻¹
 k_2 – membrane exit rate constant, min⁻¹
 k_{1d} – membrane entrance rate constant, min⁻¹
 k_{2a} – membrane exit rate constant, min⁻¹
 k_{2m} – membrane exit rate constant, min⁻¹
 R_a – reduced nitrite ion concentration in acceptor phase, dimensionless
 R_d – reduced nitrite concentration in donor phase, dimensionless
 R_m – reduced nitrite concn. in organic (memb.) phase, dimensionless
 R – reduced nitrite ion concentration, dimensionless
 $R_{m,\text{max}}$ – max. reduced nitrite ion concn. in membrane phase, dimensionless
 $S_{\text{dp/mem}}$ – interface surface of donor phase over per unit of membrane, cm²
 $S_{\text{ap/mem}}$ – interface surface of acceptor phase over per unit of membrane, cm²
 t – time, (min)
 t_{max} – time which nitrite ions concentration becoming maximum, min
 T – temperature, K
 TOACl – tetraoctyl ammonium chloride
 δ_i – distance between phases, cm
 λ – wave length of UV spectrum, nm
 ρ – density, g dm⁻³
 ϵ – extinction coefficient of UV spectrum
 φ – volume fraction, %
 ω – stirring speed, rpm
 ω_a – stirring speed of acceptor phase, rpm
 ω_d – stirring speed of donor phase, rpm
 ω_m – stirring speed of organic (membrane) phase, rpm

Subscripts

- a – acceptor phase
d – donor phase
d₀ – initial ion concentration of nitrite
m – membrane phase

References

1. *Winston Ho, W. S. and Sirkar, K. K.*, Membrane Handbook, Chapman-Hall, New York 1992
2. *Noble, R. D. and Way, J. D.*, Liquid Membrane Technology an Overview. In Liquid Membranes Theory and Applications, ACS Symp. Ser no.347, Washington, DC. 1989
3. *Mulder, M.*, Basic Principles of Membrane Technology, Kluwer Academic Publishers, Netherlands 1991
4. *Molnar, W. J.; Wang, C. P., Evans, D. F. and Cussler, E. L.*, J. Mem. Sci., **4** (1978) 129
5. *Sugiura, M. and Yamaguchi, T.*, Nippon Kagaku Kaishi, **6** (1983) 854
6. *Dahab, F. M.*, Nitrite Treatment Methods: An Overwiev., NATO ASI Series, G30, (1992) 289
7. *Patterson, J. W.*, Industrial Wastewater Treatment Technology, Butterworth Publishers, 1985 pp. 466
8. *Francis, C. W. and Callahan, M. W.*, J. Environ. Quality, **4** (1975) 153
9. *İldiz, E.*, et al., Surfactant-enhanced crossflow filtration in nitrate removal from water, ICheEng, Trans. ICheEng, **74** (1996) 546
10. *Kobyas, M.*, Transport kinetics of thiocyanate ions from aqueous environment with liquid membranes, PhD. thesis, Atatürk University, Erzurum, Turkey (1996).
11. *Fyles, T. M., Malik-Diemer, V. A. and Whitfield, D. M.*, Membrane transport systems II: Transport of alkali metal ions against their concentration gradients, Can. J. Chem., **59** (1981) 1734
12. *Szpakowska, M. and Nagy, O.B.*, Membrane material effect on copper coupled transport through liquid membranes, J. Membrane Sci., **64** (1991) 129
13. *Demircioğlu, N.*, Coupled transport kinetic of nitrate and nitrite ions from aqueous environment with liquid membranes, PhD Thesis, Atatürk University, Erzurum, Turkey (1996).
14. *Danesi, P. R.; Chiarizia, R. and Vandegrift, G. F.*, J. Phys. Chem., **84** (1980) 3455.
15. *Albery, W. J. and Choudhery, R. A.*, J. Phys. Chem., **92** (1988) 1142
16. *Szpakowska, M.*, J. Mem.Sci., **90** (1994) 101
17. *Akiba, K. and Freiser, H.*, Anal. Chim. Acta., **136** (1982) 329